

See discussions, stats, and author profiles for this publication at: <https://www.researchgate.net/publication/357330352>

# Structural Transformations and Valence States of Fe in Substituted Strontium Ferrite $\text{Sr}_2\text{LaFe}_3\text{O}_9 - \delta$

Article in *Journal of Surface Investigation X-ray Synchrotron and Neutron Techniques* · November 2021

DOI: 10.1134/S1027451021060173

CITATIONS

0

READS

4

5 authors, including:



V. Sedykh

Institute of Solid State Physics RAS

62 PUBLICATIONS 297 CITATIONS

[SEE PROFILE](#)



O. G. Rybchenko

Institute of Solid State Physics RAS

33 PUBLICATIONS 197 CITATIONS

[SEE PROFILE](#)



Valery Kulakov

Institute of Solid State Physics RAS

60 PUBLICATIONS 406 CITATIONS

[SEE PROFILE](#)

# Structural Transformations and Valence States of Fe in Substituted Strontium Ferrite $\text{Sr}_2\text{LaFe}_3\text{O}_{9-\delta}$

V. D. Sedykh<sup>a,\*</sup>, O. G. Rybchenko<sup>a</sup>, N. V. Barkovskii<sup>a</sup>, A. I. Ivanov<sup>a</sup>, and V. I. Kulakov<sup>a</sup>

<sup>a</sup> Institute of Solid State Physics, Russian Academy of Sciences, Chernogolovka, 142432 Russia

\*e-mail: sedykh@issp.ac.ru

Received April 19, 2021; revised May 21, 2021; accepted May 25, 2021

**Abstract**—The structural features and valence states of Fe in substituted strontium ferrite  $\text{Sr}_2\text{LaFe}_3\text{O}_{9-\delta}$  after a series of annealing events in vacuum at different temperatures from 400°C to 650°C are studied by X-ray diffraction (XRD) and Mössbauer spectroscopy. According to X-ray data, the two samples with extreme (in terms of oxygen content) compositions ( $\text{Sr}_2\text{LaFe}_3\text{O}_9$  and  $\text{Sr}_2\text{LaFe}_3\text{O}_8$ ) are single phase and have a rhombohedral and orthorhombic structure, respectively. When a vacancy appears, the structural state changes, multiphase states are formed, and an intermediate orthorhombic phase close to the structure of non-substituted  $\text{Sr}_4\text{Fe}_4\text{O}_{11}$  arises. The ratio of phase contents in the mixture changes as the oxygen content decreases. When an oxygen-vacancy concentration reaches one vacancy per three perovskite unit cells, the final orthorhombic phase  $\text{Sr}_2\text{LaFe}_3\text{O}_8$  is formed. According to the obtained Mössbauer data, Fe ions in the sample  $\text{Sr}_2\text{LaFe}_3\text{O}_9$  with a rhombohedral structure have two valence states:  $\text{Fe}^{4+}$  with an octahedral symmetric oxygen environment and an averaged-valence state  $\text{Fe}^{3.5+}$ . The sample  $\text{Sr}_2\text{LaFe}_3\text{O}_8$  with an orthorhombic structure, according to Mössbauer data, is magnetic; the iron ion has the  $\text{Fe}^{3+}$  valence state with two oxygen environments, octahedral and tetrahedral, as in the brownmillerite phase of unsubstituted  $\text{Sr}_2\text{Fe}_2\text{O}_5$ . Analysis of the complete data set of Fe valence states, their redistribution as the oxygen concentration decreases, and transitions from the paramagnetic state to the magnetic-ordering state allows us to correlate the information on the local environment of Fe cations with structural data.

**Keywords:** substituted perovskite-like oxides, phase transitions, Fe valence states, X-ray diffraction, Mössbauer spectroscopy

**DOI:** 10.1134/S1027451021060173

## INTRODUCTION

Substituted perovskite-like oxides have a wide range of applications: from the possibility of their use as cathode materials in fuel power engineering to spintronics, optoelectronics and microelectronics [1–3]. Recently, there have been publications on the high antibacterial properties of these compounds [4]. From the scientific and applied points of view, it is important to know the effect of the oxygen content (the appearance of vacancies) on the structure and properties of these oxides.

The partial substitution of  $\text{Sr}^{2+}$  for  $\text{La}^{3+}$  in the basic unsubstituted  $\text{SrFeO}_{3-\delta}$  oxide ( $\text{Sr}_{1-x}\text{La}_x\text{FeO}_{3-\delta}$ ) changes the oxygen content and leads to an increase in the Néel temperature [5]. The introduction of oxygen vacancies into the lattice during vacuum annealing can cause phase transformations and the appearance of various magnetic structures. The magnetic properties of these compounds are the result of a superexchange mechanism involving 3d electrons of transition-metal

ions and *p* orbital of oxygen [6], i.e., oxygen plays a very important role here.

According to [7], there are three phase regions in  $\text{La}_{1-x}\text{Sr}_x\text{FeO}_{3-\delta}$  as a function of *x*: orthorhombic ( $0 < x < 0.2$ ), rhombohedral ( $0.3 < x < 0.5$ ), and cubic ( $0.6 < x < 1.0$ ). In other works [5, 8–11], it is indicated that at  $x = 2/3$  the compound has a rhombohedral structure; in publications, there is still no unique point of view on the structural state of these compounds. This is explained by the fact that there is slight compression along one of the spatial diagonals of the cubic cell in the rhombohedral modification. The proximity to a cubic lattice (low distortion) is most likely the reason for ambiguity in the definition of the structure.

The analysis of published data shows that, as a rule, the methods for preparing samples differ [5, 8, 10–13], therefore it is very difficult to compare the results.

In this work, the structural features and iron valence states in substituted strontium ferrite  $\text{Sr}_2\text{LaFe}_3\text{O}_{9-\delta}$  after different heat-treatment condi-

**Table 1.** Structure of  $\text{Sr}_2\text{LaFe}_3\text{O}_{9-\delta}$  after different heat treatments

Sample	Phases, spatial group					
	<i>R-3c</i>		<i>Cmmm</i> , close to $\text{Sr}_4\text{Fe}_4\text{O}_{11}$		$\text{Sr}_2\text{LaFe}_3\text{O}_8$ , <i>Pmma</i>	
	cell parameters, Å	phase fractions, %	cell parameters, Å	phase fractions, %	cell parameters, Å	phase fractions, %
1300SC	$a = 5.483$ $c = 13.408$	100	—	—	—	—
400AV	$a = 5.489$ $c = 13.463$	64	$a = 11.048$ $b = 7.728$ $c = 5.510$	36	—	—
450AV	$a = 5.497$ $c = 13.567$	16	$a = 11.050$ $b = 7.729$ $c = 5.534$	52	$a = 5.519$ $b = 11.899$ $c = 5.605$	32
500AV	$a = 5.529$ $c = 13.509$	10	$a = 11.056$ $b = 7.728$ $c = 5.520$	36	$a = 5.516$ $b = 11.895$ $c = 5.605$	54
650AV	—	—	—	—	$a = 5.516$ $b = 11.894$ $c = 5.603$	100

tions are studied using X-ray diffraction and Mössbauer spectroscopy.

## EXPERIMENTAL

A polycrystalline  $\text{Sr}_2\text{LaFe}_3\text{O}_{9-\delta}$  sample was prepared by the sol-gel method in air. Strontium, iron and lanthanum nitrates in the stoichiometric ratio and glycine were used as the initial reagents. Synthesis details are described in [14]. After synthesis in air at a temperature of 1300°C, the sample was slowly cooled to room temperature together with the furnace (slow

cooling, SC). Then annealing in a vacuum chamber with a residual pressure of (AV)  $\times 10^{-3}$  Torr was carried out at temperatures of 400, 450, 500 and 650°C. Notations: 1300SC—a sample, which was synthesized at 1300°C, 400AV—a sample, which was annealed in vacuum at 400°C.

Structural certification of the samples was carried out using a Siemens-D500 diffractometer using  $\text{FeK}\alpha$  and  $\text{CoK}\alpha$  radiation. Phase analysis, the calculation of X-ray diffraction patterns, and refinement of the unit-cell parameters were performed using Powder Cell 2.4 and Match3 software.

The Mössbauer measurements were performed on a CM 1101 spectrometer operating in the constant acceleration mode using a  $^{57}\text{Co}$  (Rh) radioactive source. The Mössbauer spectra were processed using MossFit (version 3.1) and SpectrRelax software [15].

## RESULTS AND DISCUSSION

According to the X-ray data, the initial  $\text{Sr}_2\text{LaFe}_3\text{O}_{9-\delta}$  sample, which was synthesized with slow cooling (1300SC), has a rhombohedral structure (space group *R-3c*) with the unit-cell parameters  $a = 5.483$  Å and  $c = 13.408$  Å in the hexagonal setup (Table 1) or  $a = 5.475$  Å and  $\alpha = 60.07^\circ$  in the rhombohedral setup, and its diffraction pattern is given in Fig. 1. The closeness of the angle  $\alpha$  to  $60^\circ$  indicates that the unit cell is the result of a very weak distortion of the cubic structure.

The Mössbauer spectrum of the  $\text{Sr}_2\text{LaFe}_3\text{O}_{9-\delta}$  1300SC sample measured at room temperature is shown in Fig. 2a. Decomposition of the spectrum into two singlets rather than representing it with one sin-

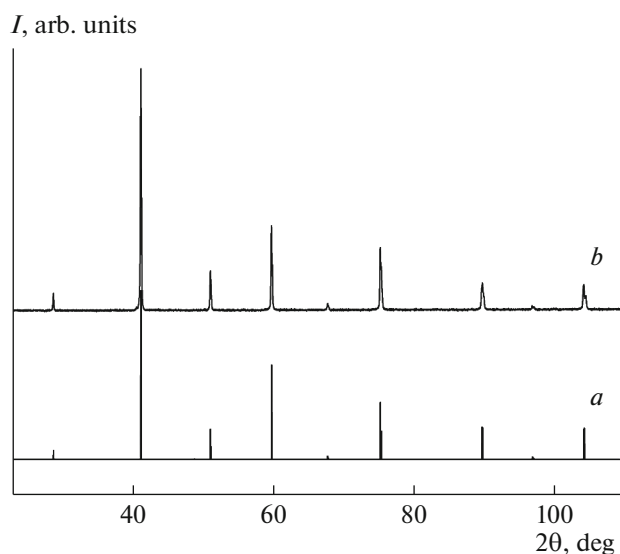


**Fig. 1.** Calculated diffraction pattern of *R-3c* (a), diffraction pattern of  $\text{Sr}_2\text{LaFe}_3\text{O}_{9-\delta}$ , 1300SC sample (b).

plet, as it might seem at first glance, gives the smallest error. The isomer shift of one singlet is typical for  $\text{Fe}^{4+}$  in the symmetric octahedral coordination. The second subspectrum corresponds to the averaged valence state  $\text{Fe}^{3.5+}$  of iron or it can be considered as an oxidation state, which can be fractional. Its isomer shift is between the corresponding shifts of  $\text{Fe}^{3+}$  and  $\text{Fe}^{4+}$ . According to [5, 12], this averaged valence state of Fe is due to the fast transfer of an electron (time constant of  $<10^{-8}$  s). The parameters of these subspectra are given in Table 2. An estimate of the oxygen content in the synthesized compound from the Mössbauer data gives the composition  $\text{Sr}_2\text{LaFe}_3\text{O}_{9.04}$ , i.e., within the error, we have an almost stoichiometric ratio for oxygen (Table 2).

The Mössbauer spectrum of the synthesized sample measured at 90 K (Fig. 2b) shows a transition to a magnetically ordered state at a decrease in temperature: the spectrum was processed by two magnetic subspectra (Table 2). A comparison of the isomer shifts of the subspectra at 300 and 90 K (Table 2) shows that the subspectrum with a larger effective magnetic field can be attributed to  $\text{Fe}^{3+}$  ions, and the subspectrum with a smaller effective magnetic field, to  $\text{Fe}^{4+}$  ions. The transition of  $\text{Fe}^{3.5+}$  into  $\text{Fe}^{3+}$  at a decrease in temperature can be explained by “freezing” the fast electron transfer.

The annealing of samples 400AV in vacuum leads to the broadening of some small-angle lines in the diffraction pattern and the appearance of weak additional lines (Fig. 3d). The processing of data shows that in addition to the rhombohedral phase, there appears a orthorhombic phase close to that of  $\text{Sr}_4\text{Fe}_4\text{O}_{11}$  of the main compound. The same additional phase was observed earlier in [5], which was called the “tetragonal” phase by the authors conditionally ( $a = 3.910 \text{ \AA}$ ,  $c = 3.867 \text{ \AA}$ ). However, in our case, description of this additional phase by a model close to  $\text{Sr}_4\text{Fe}_4\text{O}_{11}$  gives good agreement with the experiment. The lattice parameters of this phase and its fraction in the two-phase mixture are given in Table 1. When the temperature of annealing in vacuum increases, 450AV and 500AV, the diffraction pattern demonstrates the emergence of the third phase, the orthorhombic phase of  $\text{Sr}_2\text{LaFe}_3\text{O}_8$  known in publications [16], the amount of which increases with temperature (Table 1, Figs. 3e, 3f).

The Mössbauer spectrum of the 400AV sample is shown in Fig. 4a. In addition to the paramagnetic part, there emerges a magnetic sextet with the effective magnetic field  $H_n = 42.3 \text{ T}$ , which, according to the isomer shift, corresponds to  $\text{Fe}^{3+}$ , i.e., there occurs a partial transition to the magnetic state, and the Néel temperature increases. The spectrum was also obtained at low velocities in order to reveal the fine structure of the paramagnetic part. The smallest error was shown by decomposition of the spectrum into five subspectra: singlet *S1* and doublet *D1*, corresponding

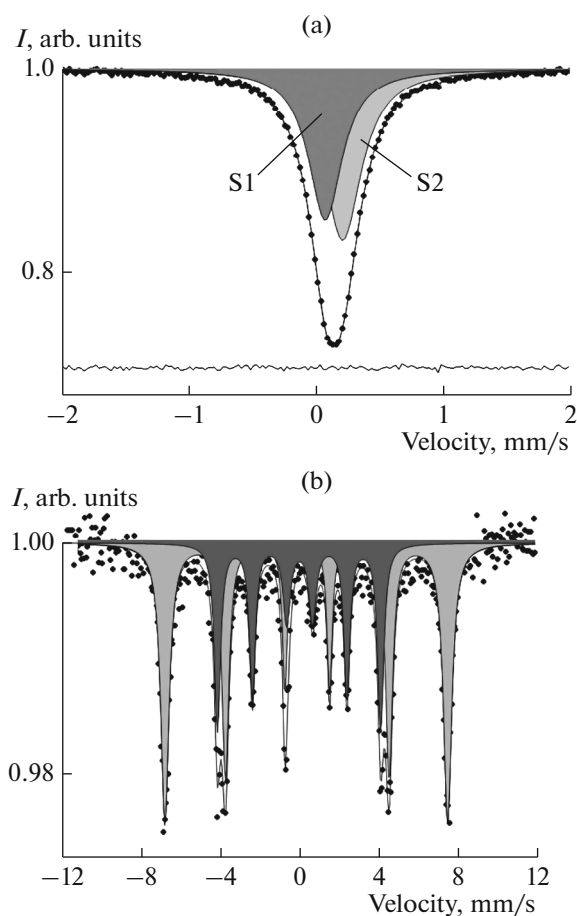


Fig. 2. Mössbauer spectra of the  $\text{Sr}_2\text{LaFe}_3\text{O}_{9-\delta}$ , 1300SC sample measured at 300 (a) and 90 K (b).

to  $\text{Fe}^{4+}$ , and doublets *D2* and *D*, corresponding to  $\text{Fe}^{3.5+}$  with different degrees of distortion of the environment, doublet *D3*, corresponding to  $\text{Fe}^{3+}$ , and a slight contribution (3%) of *D4* from two internal sextet lines. The parameters of the subspectra are given in Table 2. Taking into account the obtained X-ray data, the subspectra, corresponding to  $\text{Fe}^{3+}$ , can be attributed to the orthorhombic phase close to  $\text{Sr}_4\text{Fe}_4\text{O}_{11}$ . The amount of the paramagnetic phase in the samples decreases considerably with a temperature increase (Fig. 4b). The magnetic part consists of three subspectra: a magnetic sextet with  $H_n = 42.4 \text{ T}$  corresponding to  $\text{Fe}^{3+}$ , and two sextets looking like spectra of the brownmillerite phase of unsubstituted  $\text{Sr}_2\text{Fe}_2\text{O}_5$ , in which  $\text{Fe}^{3+}$  has two local oxygen environments: octahedral and tetrahedral [14] (Table 2). Taking into account the X-ray data, these two sextets can be attributed to the orthorhombic phase of  $\text{Sr}_2\text{LaFe}_3\text{O}_8$ , the amount of which increases greatly with temperature. Based on the Mössbauer data, the estimate of the oxygen amount in samples 400AV, 450AV and 500AV

**Table 2.** Mössbauer parameters subspectra at a temperature of 300 and 90 K of the  $\text{Sr}_2\text{LaFe}_3\text{O}_{9-\delta}$  samples

Sample	Fe valence	$T = 300 \text{ K}$				Oxygen content, $9 - \delta$
		IS	$\Delta$	$H_n$	A	
1300SC	4 + ( <i>S</i> 1)	0.04	—	—	46	9.04(2)
	3.5 + ( <i>S</i> 2)	0.18	—	—	54	
400AV	4 + ( <i>S</i> 1)	0.07	—	—	15	8.73(2)
	4 + ( <i>D</i> 1)	0.05	0.23	—	23	
	3.5 + ( <i>D</i> 2)	0.16	0.77	—	16	
	3.5 + ( <i>D</i> 2')	0.17	1.18	—	6	
	3 + ( <i>D</i> 3)	0.32	0.17	—	18	
	3 + ( <i>S</i> x1)	0.34	0.77	423	22	
450AV	4 + ( <i>D</i> 1)	−0.02	0.53	—	30	8.46(2)
	3 + ( <i>S</i> x1)	0.30	0.82	424	35	
	3 + (O) ( <i>S</i> x2)	0.34	0.37	508	24	
	3 + (T) ( <i>S</i> x3)	0.26	−0.84	388	11	
500AV	4 + ( <i>D</i> 1)	−0.01	0.65	—	15	8.33(2)
	3 + ( <i>S</i> x1)	0.27	0.81	424	31	
	3 + (O) ( <i>S</i> x2)	0.31	0.38	510	36	
	3 + (T) ( <i>S</i> x3)	0.14	−0.71	376	18	
650AV	4 + ( <i>D</i> 1)	0.09	0.35	—	3	8.00(2)
	3 + (O) ( <i>S</i> x2)	0.33	0.39	510	65	
	3 + (T) ( <i>S</i> x3)	0.15	−0.71	375	32	
90 K						
1300SC	4+	0	0.03	255	36	—
	3+	0.37	0.05	442	64	—

IS— isomer shift (with respect to BCC Fe at 300 K), mm/s;  $\Delta$ —quadrupole splitting, mm/s;  $H_n$ —effective magnetic field on the  $^{57}\text{Fe}$  nucleus, kOe; A—contribution of this subspectrum, %. *S*, *D*, *S*x—singlet, doublet, sextet, respectively, (O)—octahedral environment, (T)—tetrahedral environment.

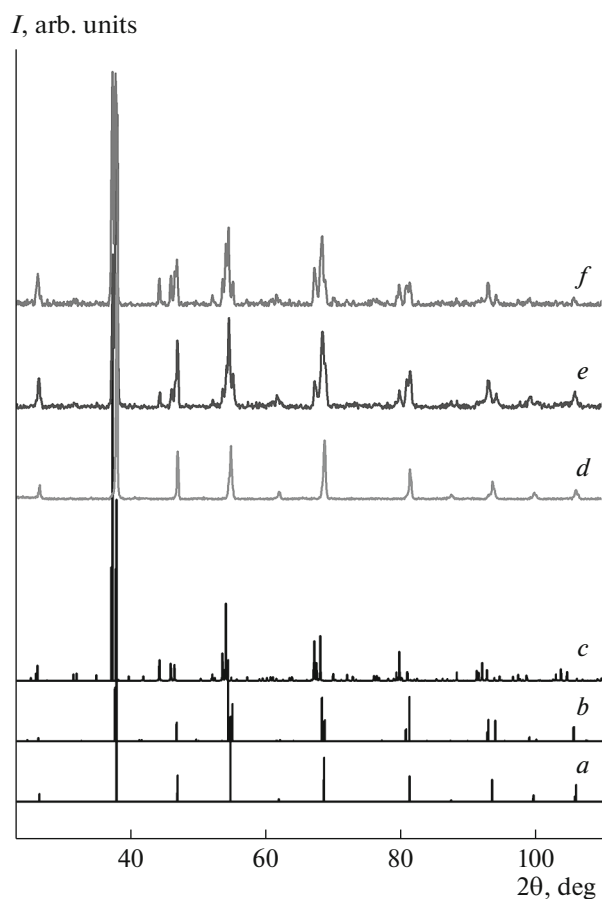


**Fig. 3.** Calculated diffraction patterns of: *a*—*R-3c*, *b*—*Cmmm* close to  $\text{Sr}_4\text{Fe}_4\text{O}_{11}$ , *c*— $\text{Sr}_2\text{LaFe}_3\text{O}_8$ ; diffraction patterns of the sample annealed in vacuum: *d*—400AV, *e*—450AV, *f*—500AV.

gives  $\text{Sr}_2\text{LaFe}_3\text{O}_{8.73}$ ,  $\text{Sr}_2\text{LaFe}_3\text{O}_{8.46}$  and  $\text{Sr}_2\text{LaFe}_3\text{O}_{8.33}$ , respectively, see Table 2.

The diffraction pattern of the 650AV sample annealed in vacuum (Fig. 5) shows the formation of the pure orthorhombic phase of  $\text{Sr}_2\text{LaFe}_3\text{O}_8$  with the lattice parameters  $a = 5.516 \text{ \AA}$ ,  $b = 11.894 \text{ \AA}$ ,  $c = 5.603 \text{ \AA}$ .

The Mössbauer spectrum of the 650AV sample is given in Fig. 6. The spectrum consists of two magnetic subspectra and a small (4%) paramagnetic additive, the parameters of which are given in Table 2, i.e., annealing in vacuum 650AV leads to a transition to a magnetically ordered phase, in which trivalent iron  $\text{Fe}^{3+}$  has two oxygen environments: octahedral and tetrahedral, the same as in  $\text{Sr}_2\text{Fe}_2\text{O}_5$  (Table 2). Estimation of the oxygen amount in the 650AV sample yields  $\text{Sr}_2\text{LaFe}_3\text{O}_8$ .

Thus, it follows from the obtained data that two samples with extreme compositions in terms of oxygen content  $\text{Sr}_2\text{LaFe}_3\text{O}_9$  and  $\text{Sr}_2\text{LaFe}_3\text{O}_8$  are single phase, i.e., when one vacancy appears per three perovskite

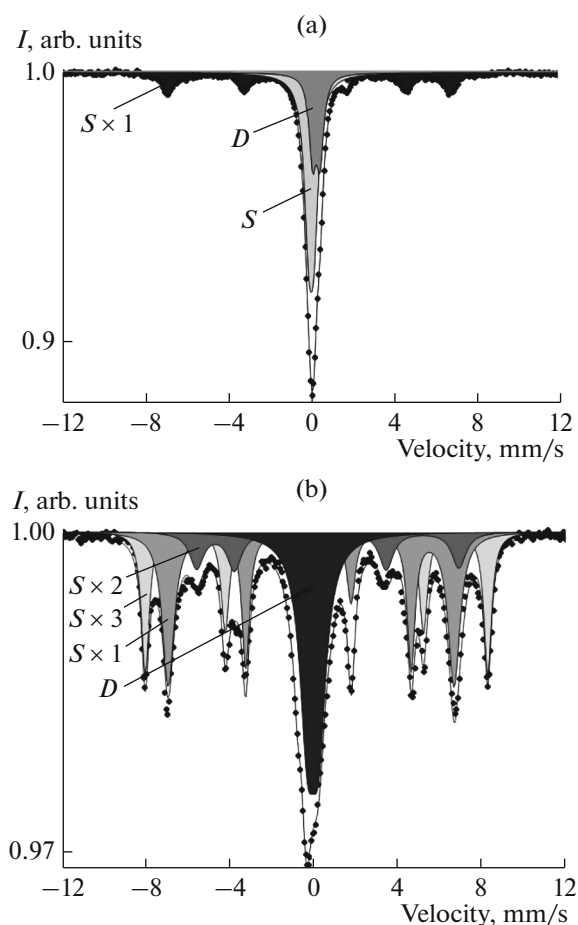


**Fig. 4.** Mössbauer spectra of *a*—400AV, *b*—450AV.

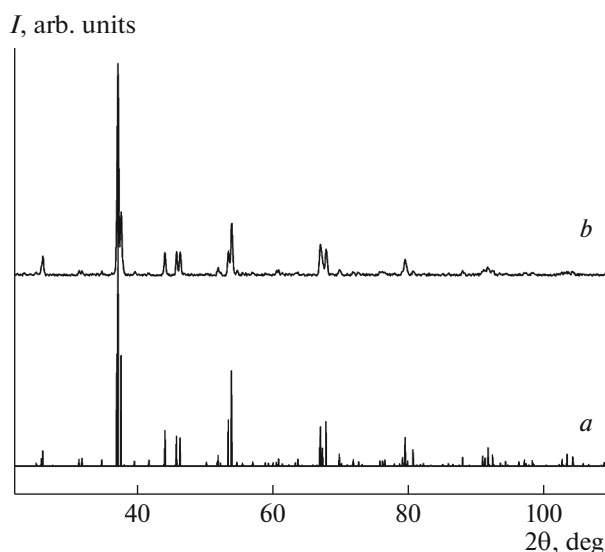


**Fig. 5.** Calculated diffraction pattern of  $\text{Sr}_2\text{LaFe}_3\text{O}_8$ , *Pmma* (*a*), diffraction pattern of the 650AV sample (*b*).

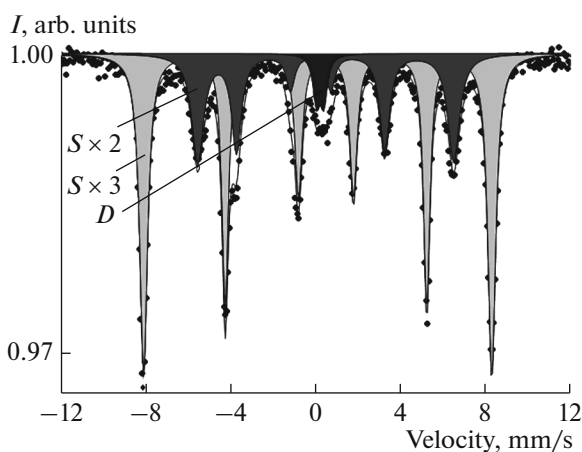


Fig. 6. Mössbauer spectrum of the 650AV sample.

cells, the  $\text{Sr}_2\text{LaFe}_3\text{O}_8$  phase is formed. The rest of the samples with intermediate oxygen states are not single phase and are a mixture of phases. The number of additional orthorhombic phases, close to the  $\text{Sr}_4\text{Fe}_4\text{O}_{11}$  phase, reaches a maximum in the region of the  $\text{Sr}_2\text{LaFe}_3\text{O}_{8.5}$  composition, then it begins to decrease. The orthorhombic phase  $\text{Sr}_2\text{LaFe}_3\text{O}_8$  appears in the same region of the composition.

With the help of Mössbauer data, it is possible to identify rather accurately only the phase  $\text{Sr}_2\text{LaFe}_3\text{O}_8$ , in which the iron valence, its environment and hyperfine fields at the iron nuclei differ from all other phases. Difficulties in identifying other phases arise because in different phases there can be the same iron valence states, and the error during identification of the phase composition increases.

### CONCLUSIONS

The structural features and iron valence states in substituted strontium ferrite  $\text{Sr}_2\text{LaFe}_3\text{O}_{9-\delta}$  have been studied by X-ray diffraction and Mössbauer spectroscopy as a function of heat-treatment conditions (annealing in a vacuum chamber with a residual pressure of  $10^{-3}$  Torr) at temperatures of 400–650°C. The substitution of 33% Sr for La leads to an increase in the oxygen amount in the synthesized sample to a stoichiometric composition and, consequently, to a decrease in the distortion of the environment of iron atoms.

A series of annealing events in vacuum at different temperatures made it possible to trace the character of the transition from one single-phase structure  $\text{Sr}_2\text{LaFe}_3\text{O}_9$  to another  $\text{Sr}_2\text{LaFe}_3\text{O}_8$  with a change in the oxygen content, to study the redistribution of iron valence states, and magnetic transitions from the paramagnetic state to the magnetically ordered one.

### REFERENCES

1. A. Lan and A. S. Mukasyan, *J. Phys. Chem.* **111**, 9573 (2007).
2. Y. Wang, J. Chen, and X. Wu, *Mater. Lett.* **49**, 361 (2001).
3. C. Yin, Q. Liu, R. Decourt, M. Pollet, et al., *J. Solid State Chem.* **184**, 3228 (2011).
4. E. K. Abdel-Khalek, D. A. Rayan, A. Askar Ahmed, M. I. A. Abdel Maksoud, and H. H. El-Bahnasawy, *J. Sol-Gel Sci. Technol.* **97**, 27 (2021). <https://doi.org/10.1007/s10971-020-05431-8>
5. P. D. Battle, N. C. Gibb, and S. Nixon, *J. Solid State Chem.* **79**, 75 (1989).
6. J. B. Goodenough, in *Progress in Solid State Chemistry*, Ed. by H. Reiss (Pergamon, London, 1971), **Vol. 5**, p. 145.
7. P. K. Gallagher and J. B. MacChesney, *Symp. Faraday Soc.* **1**, 40 (1967).
8. P. D. Battle, T. C. Gibb, and P. Lightfoot, *J. Solid State Chem.* **84**, 271 (1990).
9. M. Takano, J. Kawachi, N. Nakanishi, and Y. Takeda, *J. Solid State Chem.* **39**, 75 (1981).
10. J. B. Yang, W. B. Yelon, and W. J. James, *Phys. Rev. B: Condens. Matter Mater. Phys.* **66**, 184415 (2002).
11. T. Saha-Dasgupta, Z. S. Popovic, and S. Satpathy, *Phys. Rev. B: Condens. Matter Mater. Phys.* **72**, 045143 (2005).
12. P. D. Battle, T. C. Gibb, and S. Nixon, *J. Solid State Chem.* **77**, 124 (1988).
13. R. B. da Silva, J. M. Soares, A. P. da Costa José, J. H. de Araujo, A. R. Rodrigues, and F. L. A. Machado, *J. Magn. Magn. Mater.* **466**, 306 (2018).
14. V. D. Sedykh, O. G. Rybchenko, A. N. Nekrasov, I. E. Koneva, and V. I. Kulakov, *Phys. Solid State* **61**, 1099 (2019).
15. M. E. Matsnev and V. S. Rusakov, *AIP Conf. Proc.* **1489**, 178 (2012).
16. P. D. Battle, T. C. Gibb, and P. Lightfoot, *J. Solid State Chem.* **84**, 237 (1990).

Translated by L. Mosina